Analyst

ROYAL SOCIETY OF CHEMISTRY

PAPER

View Article Online
View Journal | View Issue

Cite this: *Analyst*, 2024, **149**, 5476

Imaging specific proteins in living cells with small unnatural amino acid attached Raman reporters†

Erli Cai,‡[a] Yage Chen,‡[a] Jing Zhang,‡[b] Haozheng Li,[d] Yiran Li,[a,d] Shuai Yan,[d] Zhiyong He,*[c] Quan Yuan*[c] and Ping Wang*[a,d,e]

Received 29th May 2024,
Accepted 2nd October 2024

DOI: 10.1039/d4an00758a

rsc.li/analyst

Fluorescence labeling *via* fluorescent proteins (FPs) or immunofluorescence has been routinely applied for microscopic imaging of specific proteins. However, due to these over-weight and oversized labels (*e.g.* GFP, 238 aa, 27 kDa, ~4 nm in size), the potential physiological malfunctions of the target proteins are largely underestimated in living cells. Herein, for living cells, we report a small and minimally-invasive Raman reporter (about 2 aa and <1 kDa), which can be site-specifically introduced into proteins by genetic codon expansion. After a single unnatural amino acid (UAA) is precisely incorporated into the target protein, the strained alkyne can rapidly undergo copper-free Diels–Alder cycloaddition reactions with the tetrazine-functionalized Raman reporter, which features a fine vibrational spectrum in contrast to fluorescence. In our experimental results, the UAA-based Raman tag was successfully incorporated into vimentin, histone 3.3 and huntingtin (Htt74Q) proteins in living HeLa cells and further utilized for stimulated Raman imaging. The site-specific bioorthogonal fusion of small Raman tags with intracellular proteins will pave the way for minimally-invasive protein labeling and multi-color imaging in living cells.

Introduction

Microscopic imaging of fluorescent proteins has long been utilized to observe spatial and temporal protein expression at the genetic level in live cells.[1–3] Although the brightness and redder working wavelengths of the fluorescent proteins have been significantly optimized for decades as labels, their comparatively large sizes are problematic.[3–6] Primarily, the over-weight fluorescent proteins fused at the N- or C-terminus of the target protein may significantly disturb the normal intracellular expression, localization and physiological functions of proteins in their native state, especially for those membrane-anchored ones.[7–9] Immuno-labelling is an alternative way to target specific proteins. However, the molecular size of antibodies (1300 aa, >150 kDa, 10 nm) is even larger than the typical fluorescent proteins, and in most cases they are not applicable to live cells.[10] To reduce the size of fluorescent labels, site-specific molecular tags have been widely explored.[11–14] Other than traditional fluorescent labels and imaging, Raman and stimulated Raman scattering microscopy (SRS) combined with alkyne labels emerges as a new bioorthogonal imaging method.[15–18] SRS, as a type of coherent Raman scattering microscopy, has dramatically improved the molecular imaging sensitivity of biomolecules, in contrast to the conventional Raman microscopy.[19,20] Meanwhile, the alkyne possesses unique spectroscopic characteristics in the cellular Raman-silent region (1800–2800 cm^{-1}), which enables alkynyl groups to serve as suitable labels for small biomolecules.[21–23] However, these alkyne reporters lack genetic specificity to target proteins in living cells.

In order to achieve high genetic specificity of alkynyl group, we genetically incorporate an UAA into a protein of interest (POI) by genetic code expansion, and then the strained alkyne on the UAA can rapidly undergo copper-free Diels–Alder cycloaddition reactions with the tetrazine-functionalized Raman reporter. The combination of bioorthogonal genetic codon expansion and click chemistry is usually applied to label small organic fluorophores, dyes and probes into proteins in live cells.[24–30] Peng Tao *et al.* reported in 2016 that Mm-pylRS-AF mutants (Y306A, Y384F) showed high efficiency in combination with endo-BCNK and 2′-aTCOK, which are commonly applied for fluorescent labeling of specific proteins in living

[a]*Britton Chance Center and MoE Key Laboratory for Biomedical Photonics, Wuhan National Laboratory for Optoelectronics-Huazhong University of Science and Technology, Wuhan, Hubei 430074, China. E-mail: p_wang@hust.edu.cn*
[b]*Department of Biochemistry and Molecular Biology, School of Basic Medicine, Tongji Medical College and State Key Laboratory for Diagnosis and Treatment of Severe Zoonotic Infectious Diseases, Huazhong University of Science and Technology, China*
[c]*College of Chemistry and Molecular Sciences, Key Laboratory of Biomedical Polymers of the Ministry of Education, Wuhan University, Wuhan, Hubei 430072, China. E-mail: hezy@whu.edu.cn, yuanquan@whu.edu.cn*
[d]*Changping Laboratory, Beijing 102206, China*
[e]*Huaiyin Institute of Technology, Huaian, Jiangsu 223003, China*
† Electronic supplementary information (ESI) available. See DOI: **https://doi.org/10.1039/d4an00758a**
‡ These authors contributed equally.

cells.[30] Moreover, the strained alkenes bearing cyclooctyne derivatives can react with tetrazines *via* the strain-promoted inverse-electron-demand Diels–Alder cycloaddition (SPIEDAC) reaction.[31,32] Importantly, it can bioorthogonally proceed in mammalian living cells due to the overwhelmingly rapid reaction rates without the need for metal catalysis.[33] In this work, we propose the Diels–Alder reaction between UAA bearing cyclooctyne and tetrazine containing an alkynyl reporter. Specifically, the cyclooctyne-bearing UAA (bicyclo[6.1.0] nonyne-lysine, BCNK; *trans*-cyclooct-2-en-L-lysine, TCOK) and the synthesized tetrazine-bearing compound containing bisarylbutadiyne (BADY) are selected on purpose to allow for non-toxic metal-free click chemistry, which shows outstanding biocompatibility in live cells.[34,35] The strained alkyne, cyclooctyne, exerts high reactivity toward tetrazine, as the latter is a nitrogen-containing heterocycle and thus extremely electron-deficient.[36,37] Also, the synthesized Raman reporter containing bisarylbutadiyne has a conjugated diyne structure (C≡C–C≡C), which presents intense Raman signals in SRS imaging.[38] In the subsequent biological experiments, we implemented bioorthogonal labeling of huntingtin proteins and histone 3.3 proteins in the nucleus and vimentin proteins in HeLa cells, respectively. We carried out multiplex SRS imaging of small UAA targeted proteins in live cells instead of fluorescence imaging in the conventional way.

Results

Genetic incorporation of a signal-enhanced Raman tag *via* the SPIEDAC reaction

We designed compound **1**, *N*-(4-(1,2,4,5-tetrazine-3-yl)benzyl)-4-(phenylbuta-1,3-diyn-1-yl) benzamide (^{1}H HMR spectrum in ESI Fig. 1,† ^{13}C HMR spectrum in ESI Fig. 2,† and FT-MS spectrum in ESI Fig. 3†), and it consequently serves as an enhanced Raman tag with a sharp Raman peak at 2215 cm^{-1} (Fig. 1a and b). By genetic codon expansion with an orthogonal pyrrolysyl-tRNA synthetase (PylRS)/PyltRNA$_{CUA}$ pair from *Methanosarcina mazei*,[39,40] we genetically incorporated an unnatural amino acid (BCNK or TCOK) at the desired site of an amber stop codon (TAG).[41–43] BCNK can undergo the SPIEDAC reaction in the presence of **1** (Fig. 1a) and result in the major reaction product **2** (~0.70 kDa) labeled on the target protein for SRS imaging in living cells (schematic of the SRS system in ESI Fig. 4†). For bioorthogonal labeling, we proceeded to label vimentin-EGFP-N150TAG with tetrazine-compound **1** site-specifically inside live cells. For this purpose, we co-transfected HeLa cells with vimentin-EGFP-N150TAG plasmids and Mm-PylRS/PyltRNA$_{CUA}$ expression plasmids in the presence of 1 mM BNCK for at least 24 h. 5 μM tetrazine-compound **1** was added for 0.5 h incubation and cells were briefly washed out right before live-cell imaging (Fig. 1c).

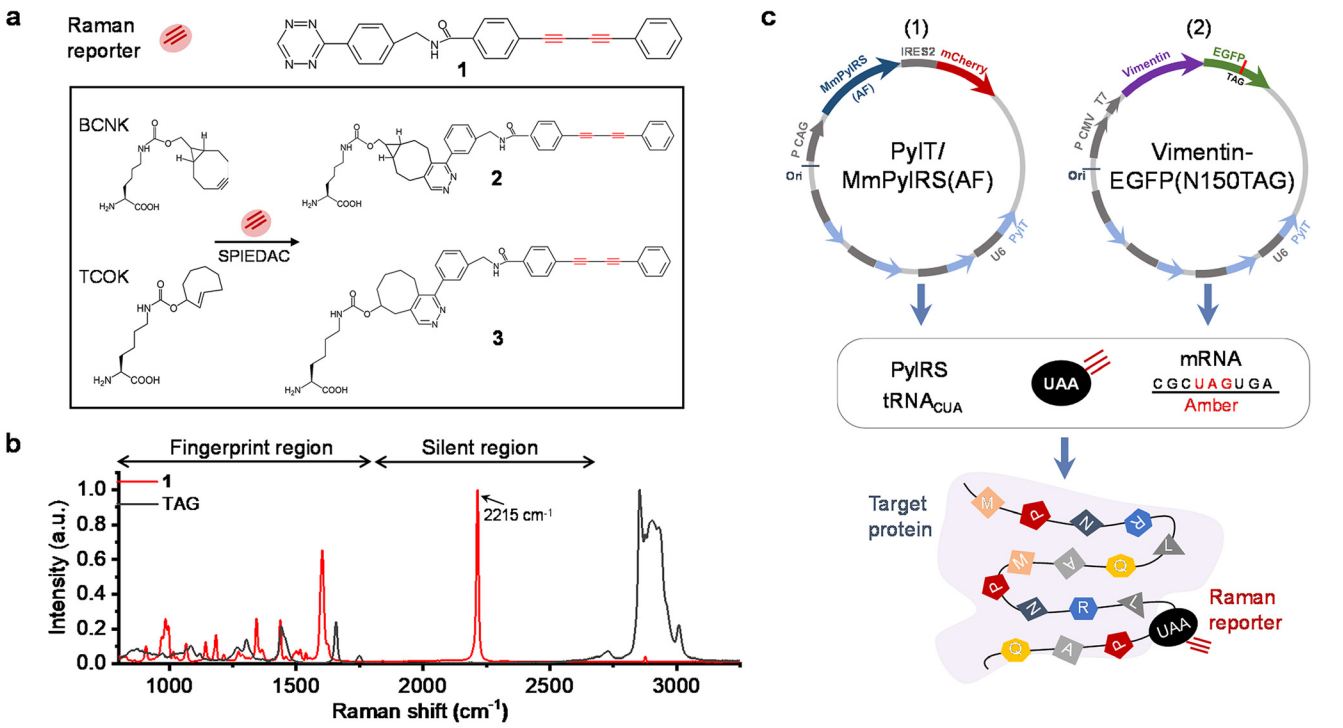

Fig. 1 Genetic incorporation of Raman tag **1** *via* genetic codon expansion and the SPIEDAC reaction. (a) Chemical structure of Raman reporter **1**; UAAs: BCNK, TCOK; Raman tags **2** and **3** formed by copper-free SPIEDAC reactions between **1** and BCNK and TCOK, respectively. (b) The spontaneous Raman spectra showed a characteristic Raman peak at 2215 cm^{-1} of Raman reporter **1**. The red and dark grey curves are Raman spectra of **1** and triacylglycerols (TAGs), respectively. TAG was used as a control, while Raman reporter **1** showed a significantly sharp Raman peak within the silent region of the spectrum in comparison with TAG. (c) Schematic diagram for site-specific labeling of POIs *via* bioorthogonal genetic code expansion and UAA-tetrazine ligation.

SRS and multiplex SRS imaging of Raman tags 2 and 3 in HeLa cells

To examine whether the designed amber-UAA-Raman tag system works, we first used BCNK for incorporation at residue N150 of EGFP, whose N-terminal is fused with vimentin, a cytoskeletal protein (Fig. 1c(2) and 2a). Meanwhile, the mCherry-tagged PylRS/Pyl-tRNA$_{CUA}$ and mutant vimentin-EGFP plasmids were co-transfected in HeLa cells (Fig. 2a). The SRS image resonant to all C–H vibrations (mainly lipids and proteins) and two-photon excited fluorescence (TPEF) image of mCherry showed that only two cells in the field of view expressed PylRS (Fig. 2b). Meanwhile, TPEF imaging of mCherry and EGFP indicated the successful expression of PylRS and vimentin in HeLa cells, respectively. In particular, multiplex SRS with resonant frequency at 2215 cm^{-1} exhibits the vibrational image of the small Raman tags (**2**) incorporated into vimentin proteins in live cells. The image localization of mCherry, SRS and GFP verifies the successful expression of both GFP and UAA labeling systems. To provide solid molecular identification of Raman reporter **2**, multiplex SRS imaging was performed with Raman shifts covering 2203–2227 cm^{-1} (Fig. 2d). The SRS spectrum obtained for vimentin (arrow in Fig. 2b) is consistent with the characteristic Raman peak of **1** (Fig. 2c), suggesting that Raman tag **2** was successfully incorporated into the amber mutant vimentin-EGFP.

We then tested the bioorthogonal Raman labeling of huntingtin and histone 3.3 proteins (Fig. 3a and c). Huntington's disease is one of the most common neurodegenerative disorders with abnormal accumulation of pathological proteins in the nucleus or cytoplasm. We constructed plasmids for transient co-transfection of Htt74Q in cells (Fig. 3a). Fig. 3b shows that only two cells had expressed PylRS and gone through the whole UAA labeling process. The SRS image shows small Raman tag **2** and the aggregation of the huntingtin proteins (GFPs) colocalized clearly. The SRS spectra of huntingtin pro-

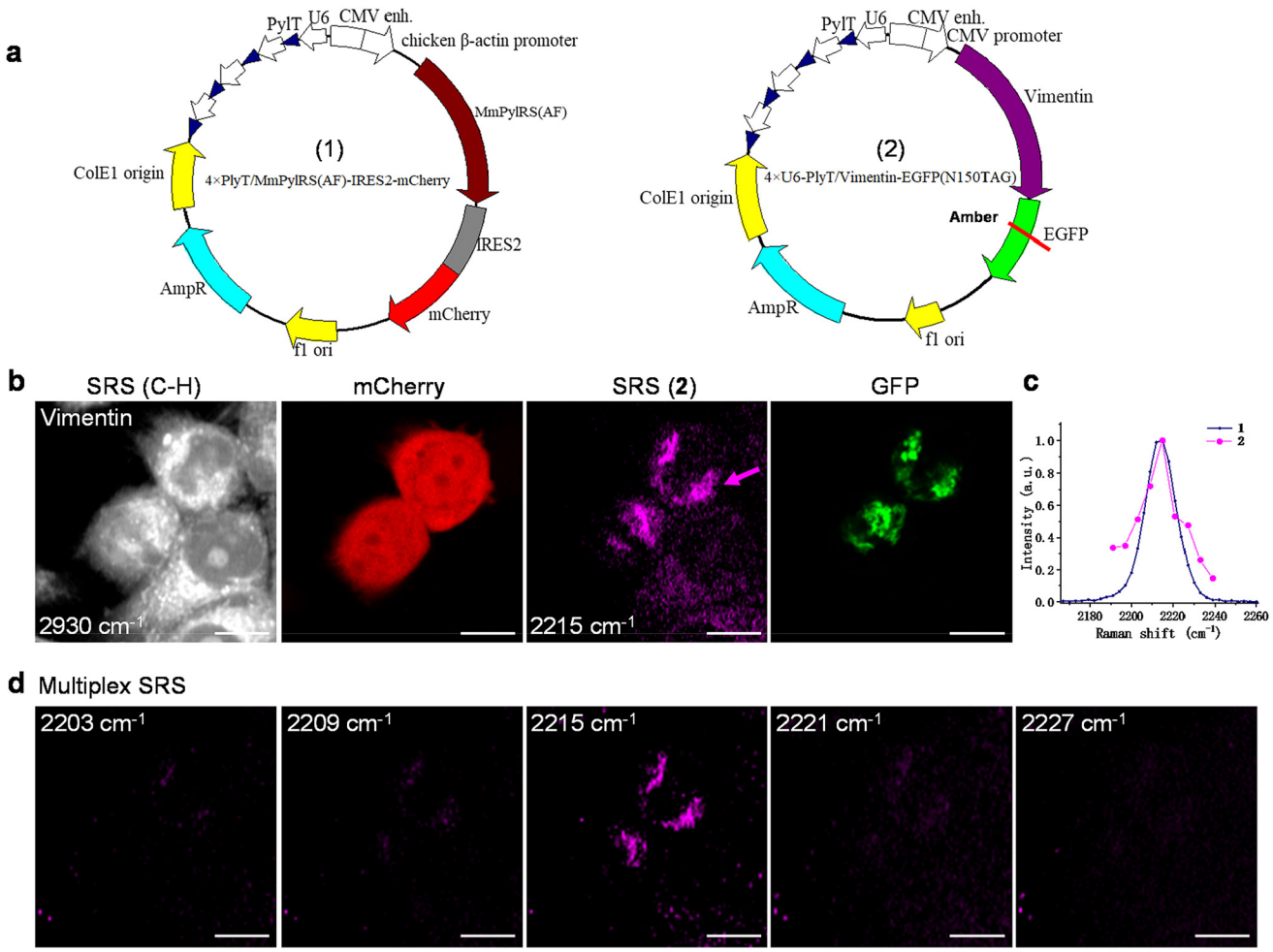

Fig. 2 SRS and multiplex SRS imaging of Raman tag **2** in living HeLa cells. (a) Structure of (1) 4 × U6-PylT/FLAG-MmPylRS-AF-IRES2-mCherry and (2) 4 × U6-PylT/vimentin-EGFP-N150TAG plasmids for transient co-transfection in HeLa cells. (b) SRS imaging of cellular lipids and proteins and TPEF imaging of MmPylRS-AF-mCherry and vimentin-EGFP fusion proteins, respectively. (c) Multiplex SRS spectra of Raman reporter **1** and vimentin proteins (magenta arrow in (b)) after background subtraction. (d) Multiplex SRS image stacks, which show the Raman reporters in vimentin-EGFP in HeLa cells. Scale bar: 15 μm.

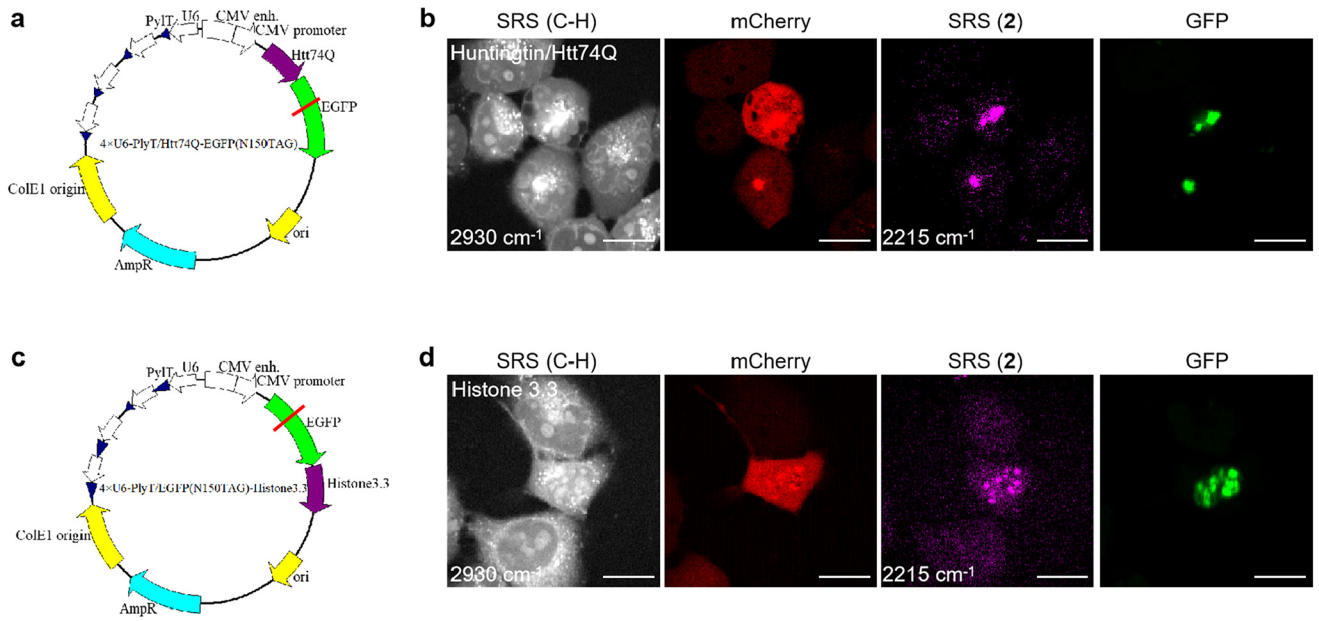

Fig. 3 Genetic incorporation of Raman tag **2** into huntingtin and histone 3.3 proteins in living HeLa cells. (a) Structure of 4 × U6-PylT/Htt74Q-EGFP-N150TAG plasmids. (b) TPEF and SRS images of huntingtin proteins. (c) Structure of the 4 × U6-PylT/EGFP-N150TAG-histone 3.3 plasmid. (d) TPEF and SRS imaging of histone 3.3 proteins in the nucleus. Scale bar: 15 μm.

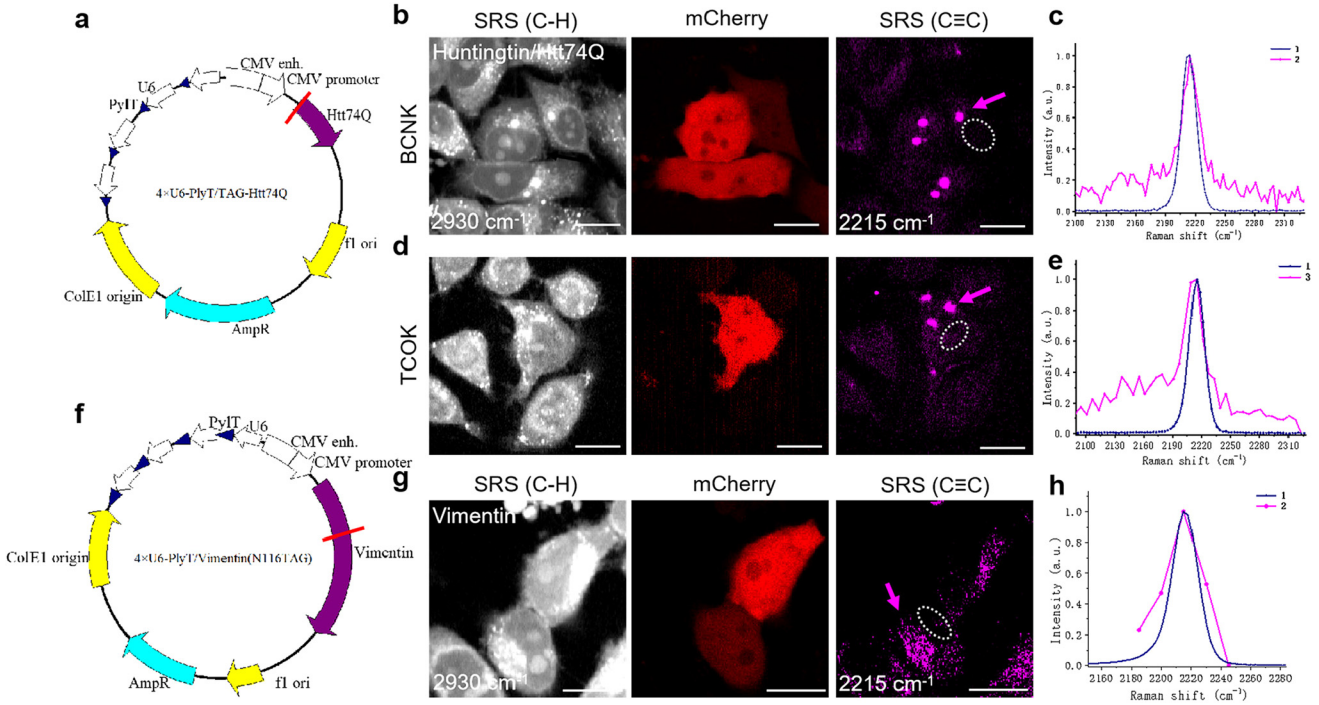

Fig. 4 Genetic incorporation of Raman reporters into specific proteins without GFPs in living HeLa cells. (a) The plasmid: 4 × U6-PylT/TAG-Htt74Q (EGFP free), for direct incorporation of an amber codon at the N-terminal of Htt74Q. (b) Multiplex SRS imaging of huntingtin and TPEF imaging of mCherry, indicating the expression of the PylRS/PyltRNACUA pair. (c) Multiplex SRS spectra obtained at the indicated location in (b) (arrow) after background subtraction (white dashed circle). SRS spectrum of **1** is shown as a reference. (d) Multiplex SRS imaging of huntingtin and TPEF imaging of mCherry, indicating the expression of the PylRS/PyltRNACUA pair. Here, we used another UAA (TCOK) for incorporation of Raman reporters. (e) SRS spectra obtained at the indicated locations in (d) (arrow). (f) The plasmid: 4 × U6-PylT/vimentin-N116TAG, for direct incorporation of an amber codon at position 116 (N116) in vimentin. (g) Multiplex SRS imaging of vimentin and TPEF imaging of mCherry, indicating the expression of the PylRS/PyltRNACUA pair. (h) SRS spectra obtained at the indicated locations (arrows) in (g). Scale bar: 15 μm.

teins are shown in ESI Fig. 5.† For a separate proof, we transfer the Raman tag to histone 3.3 proteins *via* the UAA system (Fig. 3c). In Fig. 3d and ESI Fig. 6,† the SRS observation of histone 3.3-EGFP in the nucleus was consistent with the published research studies.[38,44,45]

Incorporation of Raman tag 2 into specific proteins in the absence of GFP

In the above experiments, UAA was simply inserted into N150TAG of EGFP that targets the protein. Next, we aimed to exclude the EGFP structure and introduce Raman tag **2** into the POI directly. Specifically, we co-transfected the newly designed plasmid containing TAG-Htt74Q, in which an amber codon was directly inserted at the N-terminal of Htt74Q (Fig. 4a). In addition, another appropriate UAA, TCOK, was attempted to substitute BCNK for bioorthogonal labeling and the SPIEDAC reaction. The fluorescence images of mCherry show the expression of PylRS/$tRNA_{CUA}$ in both systems (Fig. 4b and d). Multiplex SRS spectra and images of C≡C identified the distributions of huntingtin proteins. For vimentin proteins, we inserted an amber codon at N116 of vimentin (Fig. 4f) for genetic incorporation of the Raman reporter.[30] The SRS image and SRS spectra showed clear distributions of vimentin in cells (Fig. 4g and h). In summary, we constructed an amber-UAA-Raman tag system, which successfully achieved the site-specific incorporation of a small and minimally-invasive Raman tag into specific proteins for multiplex SRS imaging in living cells.

Conclusions

We designed a small amber-UAA Raman tag system for living cells, utilizing the genetic codon expansion technology and the Diels–Alder reaction between the cyclooctyne bearing UAA and the tetrazine group in a Raman reporter. With precise incorporation of small Raman tags into the target proteins and the strong CMV promoter, we achieved stimulated Raman scattering imaging of vimentin, histone 3.3 and huntingtin Htt74Q proteins within living cells. Although the utilized SRS imaging modality already shows the best sensitivity to our Raman tag, we have not been able to perform vibrational imaging of the low-concentration proteins expressed by the normal native promoter. An UAA based Raman tag is advantageous in labeling the size and availability of colors, but Raman scattering from a Raman tag is typically more than a thousand times weaker than the fluorescence of a fluorescent protein. Thus, imaging sensitivity is the major challenge for UAA based Raman tags in the future. On the other hand, our method with quadruplet codons would possibly allow super-multiplex Raman imaging of more proteins and their interactions simultaneously in living cells.

Author contributions

E. L. C., Y. G. C., and J. Z. performed most biological and imaging experiments. Z. Y. H. synthesized the Raman reporter **1**. H. Z. L. carried out the multiplex SRS microscope system. E. L. C. analyzed the data. E. L. C., H. Z. L. and P. W. wrote the manuscript with input from all authors. P. W., Q. Y. and Z. Y. H. conceived the concept and supervised the project. We thank the Analytical & Testing Center of HUST for the Raman spectrum measurements.

Data availability

The data that support the findings of this study are available from the corresponding authors upon request. All data are incorporated into the article and its online ESI.†

Conflicts of interest

The authors declare that they have no conflicts of interest.

Acknowledgements

P. W. acknowledges the support from the National Natural Science Foundation of China (62075076), the National Key Research and Development Program of China (2016YFA0201403), the Science Fund for Creative Research Groups of China (61421064) and the Innovation Fund of the Wuhan National Laboratory for Optoelectronics.

References

1 A. Ettinger and T. Wittmann, Fluorescence live cell imaging, *Methods Cell Biol.*, 2014, **123**, 77–94.
2 D. M. Chudakov, *et al.*, Fluorescent proteins and their applications in imaging living cells and tissues, *Physiol. Rev.*, 2010, **90**(3), 1103–1163.
3 K. A. Lukyanov, Fluorescent proteins for a brighter science, *Biochem. Biophys. Res. Commun.*, 2022, **633**, 29–32.
4 S. J. Remington, Green fluorescent protein: a perspective, *Protein Sci.*, 2011, **20**(9), 1509–1519.
5 T. Haraguchi, *et al.*, Spectral imaging fluorescence microscopy, *Genes Cells*, 2002, **7**(9), 881–887.
6 M. M. Karasev, *et al.*, Near-infrared fluorescent proteins and their applications, *Biochemistry*, 2019, **84**(Suppl 1), S32–S50.
7 D. M. Chudakov, S. Lukyanov and K. A. Lukyanov, Fluorescent proteins as a toolkit for in vivo imaging, *Trends Biotechnol.*, 2005, **23**(12), 605–613.
8 E. L. Snapp, Fluorescent proteins: a cell biologist's user guide, *Trends Cell Biol.*, 2009, **19**(11), 649–655.
9 E. Snapp, Design and use of fluorescent fusion proteins in cell biology, *Curr. Protoc. Cell Biol.*, 2005, Chapter 21:21.4.1–21.4.13.
10 J. C. March, G. Rao and W. E. Bentley, Biotechnological applications of green fluorescent protein, *Appl. Microbiol. Biotechnol.*, 2003, **62**(4), 303–315.

11 I. Chen and A. Y. Ting, Site-specific labeling of proteins with small molecules in live cells, *Curr. Opin. Biotechnol.*, 2005, **16**(1), 35–40.
12 V. Thimaradka, *et al.*, Site-specific covalent labeling of His-tag fused proteins with N-acyl-N-alkyl sulfonamide reagent, *Bioorg. Med. Chem.*, 2021, **30**, 115947.
13 S. Mizukami, Y. Hori and K. Kikuchi, Small-molecule-based protein-labeling technology in live cell studies: probe-design concepts and applications, *Acc. Chem. Res.*, 2014, **47**(1), 247–256.
14 C. Jing and V. W. Cornish, Chemical tags for labeling proteins inside living cells, *Acc. Chem. Res.*, 2011, **44**(9), 784–792.
15 W. Min, *et al.*, Coherent nonlinear optical imaging: beyond fluorescence microscopy, *Annu. Rev. Phys. Chem.*, 2011, **62**, 507–530.
16 S. Hong, *et al.*, Live-cell bioorthogonal Raman imaging, *Curr. Opin. Chem. Biol.*, 2015, **24**, 91–96.
17 H. Yamakoshi, *et al.*, Alkyne-tag Raman imaging for visualization of mobile small molecules in live cells, *J. Am. Chem. Soc.*, 2012, **134**(51), 20681–20689.
18 S. Bakthavatsalam, K. Dodo and M. Sodeoka, A decade of alkyne-tag Raman imaging (ATRI): applications in biological systems, *RSC Chem. Biol.*, 2021, **2**(5), 1415–1429.
19 L. Wei, *et al.*, Live-Cell Bioorthogonal Chemical Imaging: Stimulated Raman Scattering Microscopy of Vibrational Probes, *Acc. Chem. Res.*, 2016, **49**(8), 1494–1502.
20 L. Wei, *et al.*, Imaging complex protein metabolism in live organisms by stimulated Raman scattering microscopy with isotope labeling, *ACS Chem. Biol.*, 2015, **10**(3), 901–908.
21 L. Wei, *et al.*, Live-cell imaging of alkyne-tagged small biomolecules by stimulated Raman scattering, *Nat. Methods*, 2014, **11**(4), 410–412.
22 F. Hu, L. Shi and W. Min, Biological imaging of chemical bonds by stimulated Raman scattering microscopy, *Nat. Methods*, 2019, **16**(9), 830–842.
23 S. Hong, *et al.*, Live-cell stimulated Raman scattering imaging of alkyne-tagged biomolecules, *Angew. Chem., Int. Ed.*, 2014, **53**(23), 5827–5831.
24 D. P. Nguyen, *et al.*, Genetic encoding and labeling of aliphatic azides and alkynes in recombinant proteins via a pyrrolysyl-tRNA Synthetase/tRNA(CUA) pair and click chemistry, *J. Am. Chem. Soc.*, 2009, **131**(25), 8720–8721.
25 A. Q. Hassan, Site-specific incorporation of chemical probes into proteins for NMR, *ACS Chem. Biol.*, 2008, **3**(9), 524–526.
26 A. Deiters and P. G. Schultz, In vivo incorporation of an alkyne into proteins in Escherichia coli, *Bioorg. Med. Chem. Lett.*, 2005, **15**(5), 1521–1524.
27 T. Yanagisawa, *et al.*, Multistep engineering of pyrrolysyl-tRNA synthetase to genetically encode N(epsilon)-(o-azidobenzyloxycarbonyl) lysine for site-specific protein modification, *Chem. Biol.*, 2008, **15**(11), 1187–1197.
28 M. Grammel and H. C. Hang, Chemical reporters for biological discovery, *Nat. Chem. Biol.*, 2013, **9**(8), 475–484.
29 E. M. Sletten and C. R. Bertozzi, From Mechanism to Mouse: A Tale of Two Bioorthogonal Reactions, *Acc. Chem. Res.*, 2011, **44**(9), 666–676.
30 T. Peng and H. C. Hang, Site-Specific Bioorthogonal Labeling for Fluorescence Imaging of Intracellular Proteins in Living Cells, *J. Am. Chem. Soc.*, 2016, **138**(43), 14423–14433.
31 M. L. Blackman, M. Royzen and J. M. Fox, Tetrazine ligation: fast bioconjugation based on inverse-electron-demand Diels-Alder reactivity, *J. Am. Chem. Soc.*, 2008, **130**(41), 13518–13519.
32 M. T. Taylor, *et al.*, Design and Synthesis of Highly Reactive Dienophiles for the Tetrazine-Cyclooctene Ligation, *J. Am. Chem. Soc.*, 2011, **133**(25), 9646–9649.
33 V. Slachtova, *et al.*, Bioorthogonal chemistry in cellular organelles, *Top. Curr. Chem.*, 2023, **382**(1), 2.
34 G. Zhao, *et al.*, Tetrazine bioorthogonal chemistry derived in vivo imaging, *Front. Mol. Biosci.*, 2022, **9**, 1055823.
35 Y. Deng, *et al.*, Tetrazine-isonitrile bioorthogonal fluorogenic reactions enable multiplex labeling and wash-free bioimaging of live cells, *Angew. Chem., Int. Ed.*, 2024, **63**(10), e202319853.
36 N. K. Devaraj and R. Weissleder, Biomedical applications of tetrazine cycloadditions, *Acc. Chem. Res.*, 2011, **44**(9), 816–827.
37 E. Lallana, R. Riguera and E. Fernandez-Megia, Reliable and efficient procedures for the conjugation of biomolecules through Huisgen azide-alkyne cycloadditions, *Angew. Chem., Int. Ed.*, 2011, **50**(38), 8794–8804.
38 J. Zhang, *et al.*, Small Unnatural Amino Acid Carried Raman Tag for Molecular Imaging of Genetically Targeted Proteins, *J. Phys. Chem. Lett.*, 2018, **9**(16), 4679–4685.
39 K. J. Lee, D. Kang and H. S. Park, Site-Specific Labeling of Proteins Using Unnatural Amino Acids, *Mol. Cells*, 2019, **42**(5), 386–396.
40 J. Xie and P. G. Schultz, A chemical toolkit for proteins–an expanded genetic code, *Nat. Rev. Mol. Cell Biol.*, 2006, **7**(10), 775–782.
41 I. Nikic, *et al.*, Minimal tags for rapid dual-color live-cell labeling and super-resolution microscopy, *Angew. Chem., Int. Ed.*, 2014, **53**(8), 2245–2249.
42 G. Srinivasan, C. M. James and J. A. Krzycki, Pyrrolysine encoded by UAG in Archaea: charging of a UAG-decoding specialized tRNA, *Science*, 2002, **296**(5572), 1459–1462.
43 B. Hao, *et al.*, A new UAG-encoded residue in the structure of a methanogen methyltransferase, *Science*, 2002, **296**(5572), 1462–1466.
44 C. Bergqvist, *et al.*, Monitoring of chromatin organization in live cells by FRIC. Effects of the inner nuclear membrane protein Samp1, *Nucleic Acids Res.*, 2019, **47**(9), e49.
45 M. C. Rico, *et al.*, Extracellular acetylated Histone 3.3 induces inflammation and lung tissue damage, *Biomolecules*, 2023, **13**(9), 1334.